

# High Strength Pyroxene-Based Glass- Ceramic Foams in the Presence of $\text{Fe}_2\text{O}_3$

P. Shahsavari, B. Eftekhari Yekta\* and V. K. Marghussian

\* [beftekhari@iust.ac.ir](mailto:beftekhari@iust.ac.ir)

Received: April 2020

Revised: July 2020

Accepted: August 2020

\* School of Metallurgy and Materials Engineering, Department of Ceramics, Iran University of Science and Technology, Tehran, Iran.

DOI: 10.22068/ijmse.17.3.1

**Abstract:** Strong glass-ceramic foams with a compressive strength of 20 MPa were prepared by adding various amounts of  $\text{Fe}_2\text{O}_3$  to a soda lime-based glass composition, using SiC as a foaming agent. The foams were prepared by heat treatment of the compacted samples in the range of 750–950°C and various soaking times. The crystallization behavior of the samples was investigated by Simultaneous Thermal Analysis (STA), Scanning Electron Microscope, and X-Ray Diffractometer (XRD). Based on the results, solid solutions of pyroxene groups were crystallized by the surface mechanism, between 730 and 900°C, and their amounts increased with the increase in the added iron oxide. In addition, we found that  $\text{Fe}_2\text{O}_3$  neither acts as a nucleant for pyroxene nor as an oxidizer for SiC. The results also showed that the compressive strength as well as the crystallization behavior of the foams were influenced by the presence of the SiC particles.

**Keywords:** Glass-Ceramic, Foam, Pyroxene.

## 1. INTRODUCTION

Glass foam has a unique combination of properties such as low density, suitable rigidity, thermal insulation, rodent, insect, water and steam resistance. Commercial glass foams exhibit porosity, apparent density, and compressive strength values of approximately 85 – 95 vol%, 0.1 – 0.3 g/cm<sup>3</sup>, and 0.4 – 6 MPa, respectively[1].

Manufacturing glass foam via recycling silicate industrial wastes has been popular in the last two decades. However, the reported mechanical strengths of these materials have not been satisfactorily [2-15]. To improve such a deficiency and to achieve more control on foaming behavior, researches have been conducted on manufacturing glass-ceramic foams[5,8,11,16]. But, almost none of them, namely cathode ray tube (CRT) and soda-lime glasses have met the required mechanical properties with proper relative density. This is mainly because the mentioned systems are hardly inclined to crystallize [5, 8, 11].

Transition metal oxides containing glasses seem to be appropriate candidates to make up the above-mentioned deficiency. For instance, it is said that iron oxide affects both nucleation and crystallization of silicate glasses [17-19]. Based

on various reports, multiple ion valences of iron along with alkaline oxides facilitate pyroxene formation and improve the abrasion resistance, mechanical strength and chemical durability of glasses [18, 20, 21].

Since the foaming performance of soda-lime glass in the presence of SiC particles has been approved previously, various glasses containing similar ratios of a soda-lime glass constituent, and amounts of iron oxide were melted, mixed with SiC particles, and their crystallization behavior, density and strength were evaluated. The chosen compositions were simple simulations of the well-known Iranian copper slag by-product. The authors believed that the results of this experiment could help us to have a better evaluation of the glass foams, which will produce from copper slag.

## 2. EXPERIMENTAL PROCEDURE

The chemical compositions of the glasses that will be denoted as  $G_x$  in this article are shown in Table 1. Here “X” indicates the weight of the part of iron oxide, which was present in each glass composition. In fact, the glasses are formulated based on a soda-lime glass composition; but, contain various amounts of  $\text{Fe}_2\text{O}_3$ .

**Table 1.** Chemical composition of glasses G<sub>20</sub>, G<sub>24</sub>, G<sub>28</sub>, and G<sub>32</sub> (parts weight).

|                                | G <sub>20</sub> | G <sub>24</sub> | G <sub>28</sub> | G <sub>32</sub> |
|--------------------------------|-----------------|-----------------|-----------------|-----------------|
| SiO <sub>2</sub>               | 73.84           | 73.84           | 73.84           | 73.84           |
| Fe <sub>2</sub> O <sub>3</sub> | 19.54           | 24.03           | 27.74           | 31.70           |
| CaO                            | 8.77            | 8.77            | 8.77            | 8.77            |
| Al <sub>2</sub> O <sub>3</sub> | 1.79            | 1.79            | 1.79            | 1.79            |
| MgO                            | 1.40            | 1.40            | 1.40            | 1.40            |
| Na <sub>2</sub> O              | 12.95           | 12.95           | 12.95           | 12.95           |
| K <sub>2</sub> O               | 0.97            | 0.97            | 0.97            | 0.97            |
| TiO <sub>2</sub>               | 0.28            | 0.28            | 0.28            | 0.28            |

The glass batches were melted in zircon crucible in an electric furnace at 1450 °C for 1 h. Then, the melts were quenched into cooled water. The frits were milled in a planetary mill for 20 min. The mean particle size of the frits was approximately 20 μm. The ground powders were mixed thoroughly with SiC powder (reagent grade, Sigma–Aldrich, and particle size <45 μm) and suitable amounts of PVA solution.

The amounts of SiC, which were added to the aforementioned ground frits, were 1, 2, 3, and 4%wt.

The mixed batches were uniaxially pressed under 80 MPa pressure using a hydraulic press into a 20 mm diameter cylindrical steel die. The samples were then heat-treated between 700 and 950 °C with a soaking time of 25 min and cooled to room temperature in the furnace. The heating rate was 10 °C/min.

The crushing strength was determined using specimens with 5mm×10mm×10mm dimensions.

An Instron Universal Testing Machine with a crosshead speed of 1 mm/min was used in these experiments. At least three specimens were evaluated for each composition.

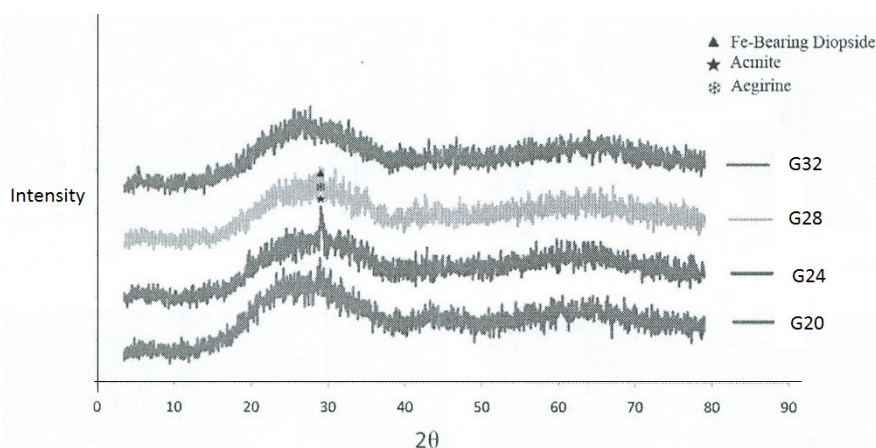
The bulk density of the cubic samples was obtained by measuring their dimensions and their true density was determined via the pycnometer. The thermal analysis was carried out by simultaneous thermal analysis (NETZSCH 409) in the air using a heating rate of 10°C/min.

The crystallinity of the samples was investigated by an X-ray diffractometer (Philips PW1800). The microstructure of the samples was studied by SEM micrographs (SEM, TESCAN), after polishing and etching of the samples, using 5% hydrofluoric acid for 60 sec.

### 3. RESULTS AND DISCUSSION

#### 3.1. Crystallization and Foaming Behaviors

Glass composition, heat treatment temperature, soaking time, the amount, and the type of foaming agent are key parameters that affect the final structure of the foamed specimens[1]. It is well known that a soda-lime glass is not very susceptible to crystallization. Surface crystallization of devitrite(Na<sub>2</sub>Ca<sub>3</sub>Si<sub>6</sub>O<sub>16</sub>) and wollastonite (CaSiO<sub>3</sub>) have been reported only in fine particles of it containing a nucleant [10]. On the other hand, the pyroxene groups easily crystallize in the high iron-bearing silicate glasses [16, 18, 22]. Therefore, to enhance crystallization in a soda-lime glass composition, the addition of iron oxide to the glass batches was considered. Being multi-valance, iron oxide can play the role of an oxidizer, and consequently it

**Fig.1.** X-ray diffraction patterns of the fritted samples.

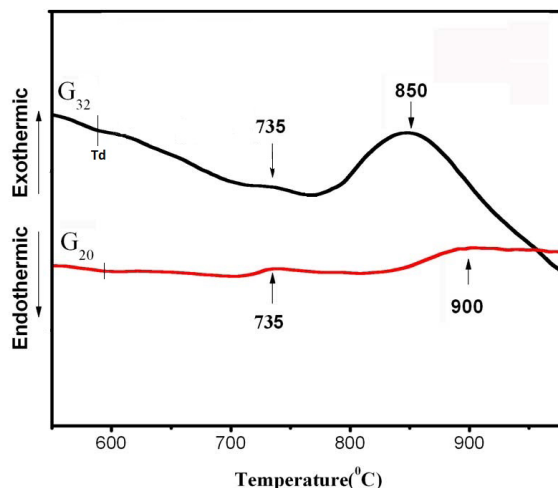
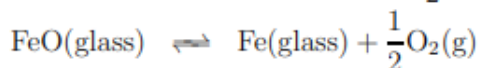
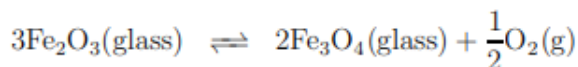


Fig. 2. DTA curves of G<sub>20</sub> and G<sub>32</sub> with a heating rate of 10°C/min.

can provide the oxidizing condition for SiC by the following reactions [3]:



Then, silicon carbide can release CO/CO<sub>2</sub> by absorbing the oxygen delivered by the mentioned redox reactions, and/or the oxygen entrapped in the pores as well as the dissolved one in the glass [3, 23].

Figs.1 and 2 show the X-ray diffraction patterns of frit samples and the DTA traces of the glasses G<sub>20</sub> and G<sub>32</sub>, containing the minimum and the maximum amounts of iron oxide, respectively. As can be seen, the glasses display an amorphous structure in XRD patterns. Also, based on fig.2, the dilatometric softening point temperature (T<sub>d</sub>) of G<sub>20</sub> and G<sub>32</sub> seems to be at approximately 590 and 585°C, respectively. There are two distinct exothermic peaks in each sample which most probably can be attributed to crystallization of glasses. While the first peak does not change with increasing of Fe<sub>2</sub>O<sub>3</sub> and remaining at approximately 735°C, the second one undergoes a significant reduction from 900 to 850°C. Furthermore, the intensity of the latter peak has increased considerably.

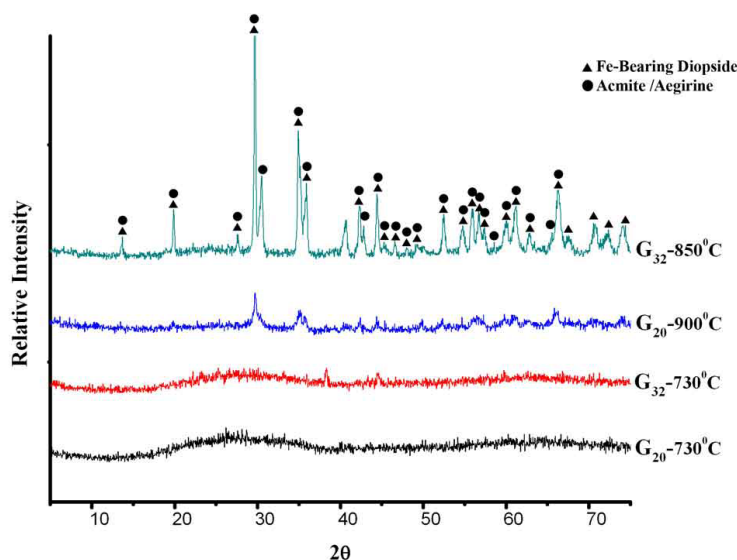
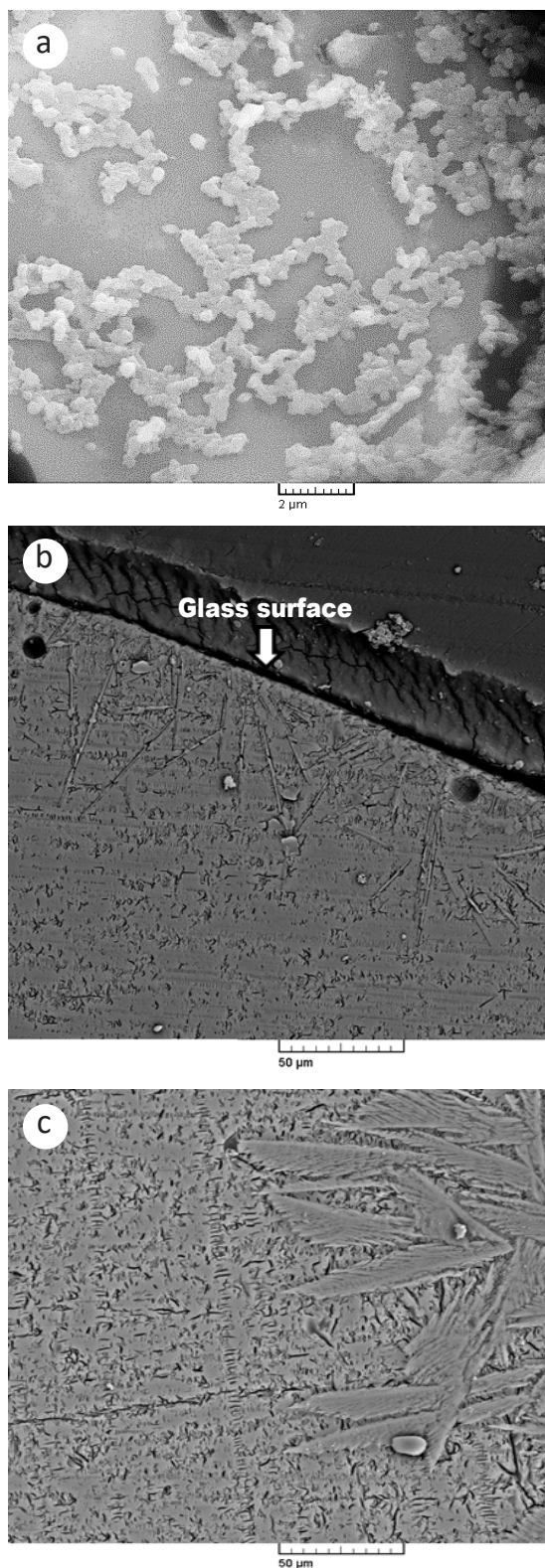


Fig. 3. XRD patterns of glasses G<sub>20</sub> and G<sub>32</sub> after heat treatment at 730°C and 900°C for 10 min.



**Fig. 4.** SEM micrograph of a) glass  $G_{20}$  after heating at  $730^{\circ}\text{C}$ , mag=10000X; B) glass  $G_{20}$  heat-treated at  $900^{\circ}\text{C}$ , mag=1000X; and C) the glass  $G_{32}$  heat-treated at  $850^{\circ}\text{C}$  for 10 min, mag=1000X.

To determine the nature of the two peaks, the samples were heat-treated at the two temperatures for 10 min (Fig.3). No crystalline phase was detected in the X-ray diffraction patterns of the samples heat-treated at the first exothermic peak for 10 min; but, many spherical micro-crystals were observed in their SEM micrographs (Fig.4-a).

Two pyroxene-based phases including a Fe-bearing diopside (the main crystalline phase) ( $\text{Fe}_{0.35}\text{Al}_{0.2}\text{Mg}_{0.44}\text{Ca}_{0.96}(\text{Fe}_{0.08}\text{Si}_{0.7}\text{Al}_{0.2})_2\text{O}_{6.12}$ ) (JCPDF #08321) as well as acmit and aegirine, were revealed in both glasses after heat treatment at their second DTA crystallization peak. Acmit and aegirine are different polymorphs of  $\text{NaFe}(\text{SiO}_3)_2$  (JCPDF #010221) and distinguishing between their XRD patterns was difficult except for some peaks.

These results are consistent with previous reports [16, 23-25]. In particular, Salman et al., Karamanov [24] and Mohamed et al.[16] have shown that high iron-containing silicate glasses mainly crystallize to solid solutions of pyroxenes. It has also been reported that pyroxene phases can be heterogeneously recrystallized on an intermediate spinel-based phase like magnetite. The initial stage of crystallization of iron-rich glasses is characterized by a liquid-liquid phase separation [18]. First, spinel-based phases, e.g. magnetite, franklinite, and/or chromite, precipitate within the iron-rich liquid phase. Afterward, they act as the nucleation site for the crystallization of pyroxene during the later heat treatment [16,18]. However, our experiments showed that magnetite was gradually disappeared with increasing of iron oxide.

Based on the XRD results (Fig.3), the intensity of the patterns has significantly increased with iron contents, which is compatible with the DTA results. The dilatometric softening point temperature ( $T_d$ ) of the two glasses is almost the same. However, glass  $G_{32}$  showed a greater tendency to crystallize. This can be attributed to the role of  $\text{Fe}_2\text{O}_3$ , which a) sometimes plays as a nucleating agent [17, 18, 26], and/ or b) is a component of the crystalline phases that its increasing leads to improvement of crystallization.

Figs. 4-b and 4-c show the cross-sectional views of SiC-free glasses  $G_{20}$  and  $G_{32}$ , respectively, shaped via the melt casting method, heat-treated at their second peak temperatures for 10 min, and then rapidly cooled. By comparing these two

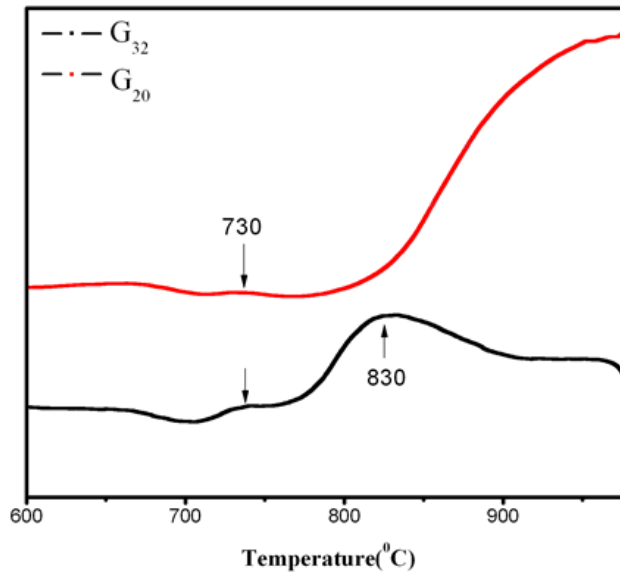


Fig. 5 - DTA curves of  $G_{20}+SiC(2\%wt)$  and  $G_{32}+SiC(2\%wt)$  with a rate of  $10^{\circ}C/min$ .

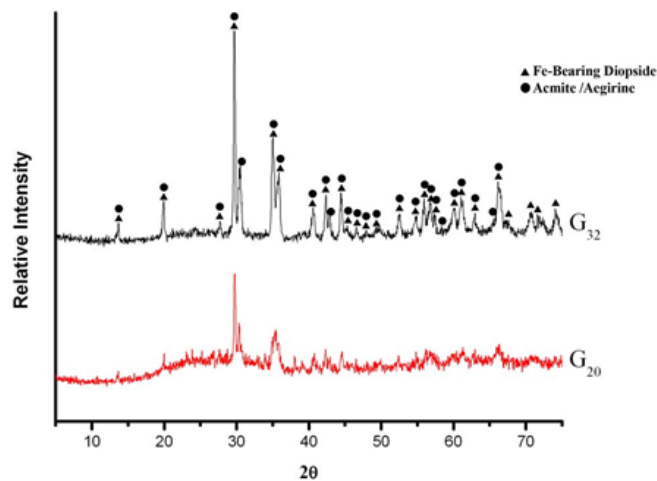


Fig. 6. X-ray diffraction patterns of glasses  $G_{20}$  and  $G_{32}$  containing 2%wt SiC fired at  $850^{\circ}C$  for 25 min.

Figs, it can be concluded that surface crystallization is the predominant mechanism for crystallization in both glasses. However, crystallization has been more rapid in  $G_{32}$  than  $G_{20}$ , as the dendritically grown crystals are larger in the former one. Based on these results, one can conclude that item (b) is likely responsible for the reduction of DTA crystallization peak temperature with iron oxide.

The addition of SiC (2 wt.%) to  $G_{20}$  and  $G_{32}$ , as a foaming agent, led to a decrease in the crystallization peak temperature of  $G_{32}$  (Fig.5). It seems that SiC particles has advanced the surface crystallization of the mentioned phases via entering new glass surfaces, through foaming of the glass,

and it did not change the types of the precipitated phases(Fig.6).

Fig.7 shows the microstructures of glass-ceramic foams  $G_{20}$ ,  $G_{24}$ ,  $G_{28}$ ,  $G_{32}$  after heat treatment at  $850^{\circ}C$  for 25 min. The pores have become more isolated and smaller with the increase of  $Fe_2O_3$ . Based on the previous equitation's,  $Fe_2O_3$  is known as an oxidizer for SiC particles, and can improve the foaming process by releasing of oxygen.

If these reactions had worked in the batch, they would have made the holes bigger. But, it seems that due to the greater crystallization in  $G_{32}$  which usually leads to an increase in glass vis-

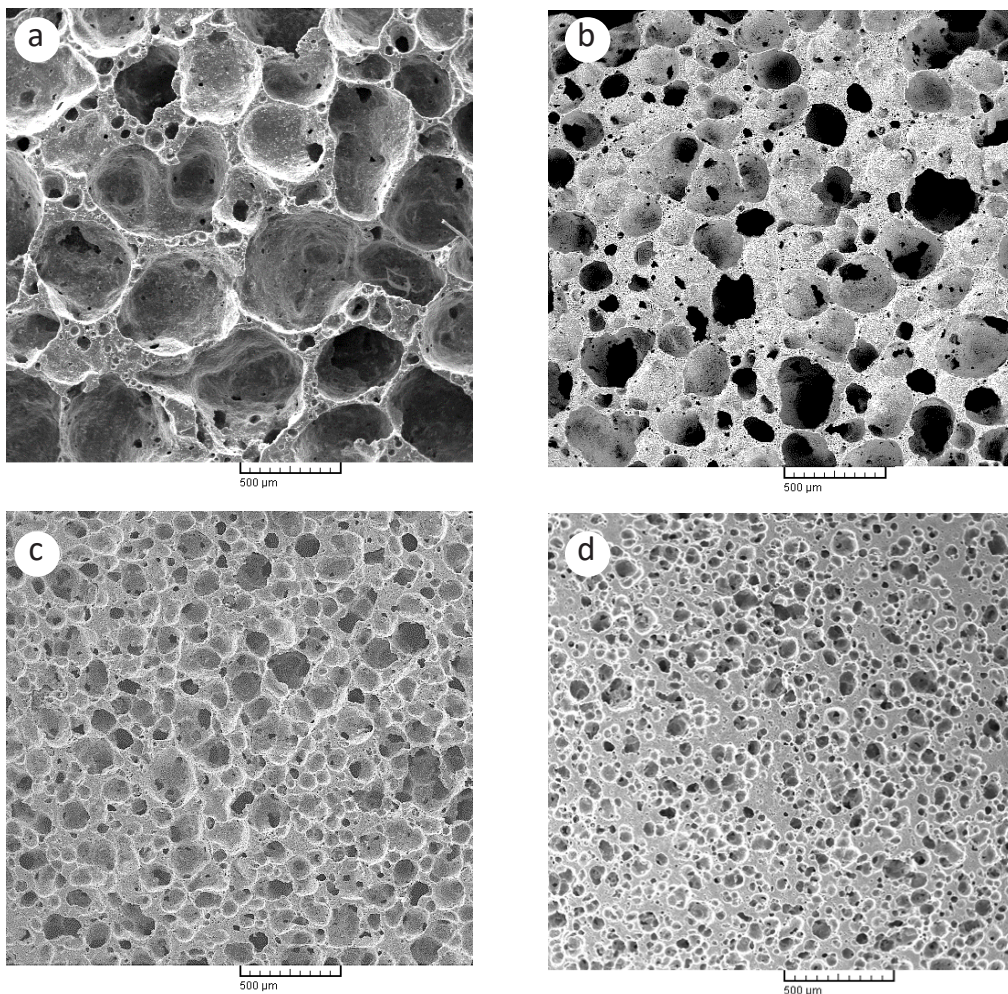


Fig. 7. SEM micrographs of a) glass G<sub>20</sub> and b) glass G<sub>24</sub> c) glass G<sub>28</sub> d) glass G<sub>32</sub> pore morphology after treatment at 850°C for 25min.

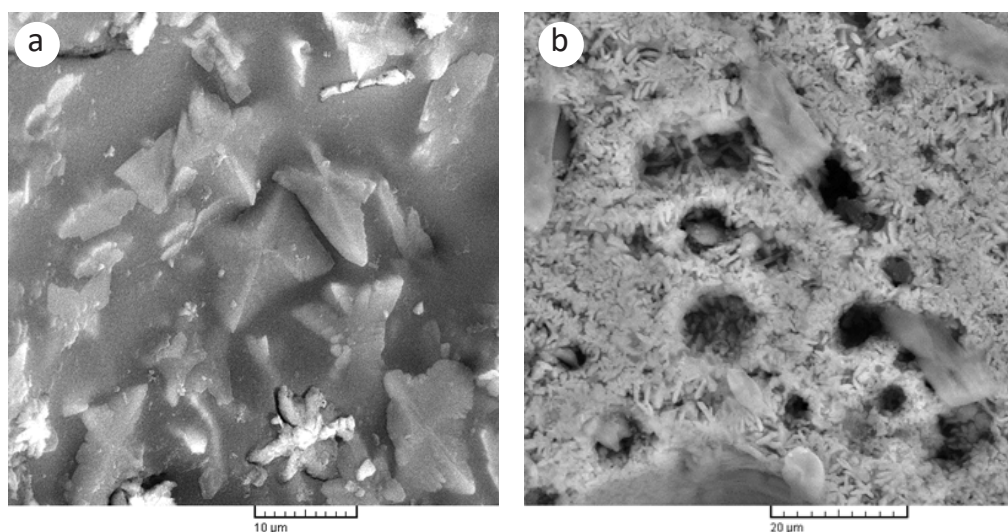


Fig. 8. The morphologies of crystalline phases in a) G<sub>20</sub>; and b) G<sub>32</sub> after heat treatment at 850°C 25min.

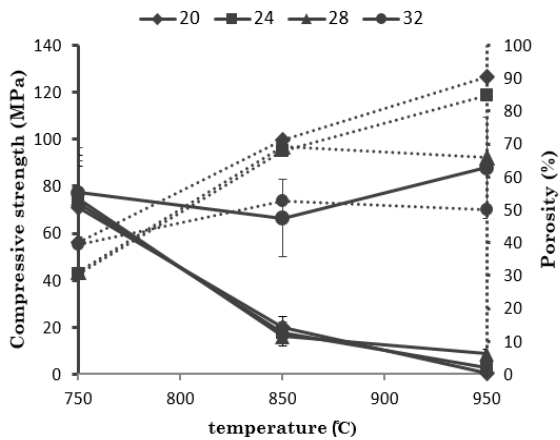


Fig. 9. Strength-porosity variation of specimens with heat treatment temperature in the presence of %2wt SiC for 25 min.

osity [27], its foaming has decreased. It should be noted that the average size of pores in samples  $G_{20}$ ,  $G_{24}$ ,  $G_{28}$ , and  $G_{32}$  is  $\sim 350$ ,  $200$ ,  $100$   $\mu\text{m}$ , and  $40$   $\mu\text{m}$ , respectively, and the surface pore density has also decreased with the same trend. Furthermore, Instead of slight prismatic crystalline phase which was precipitated in  $G_{20}$ (Fig. 8a), an extensive precipitation of needle-like small crystals are seen in the microstructure of foam prepared by  $G_{32}$ (Fig. 8b).

### 3.2. Mechanical Properties

Figs. 8 and 9 depict the variation of porosity and compressive strengths of various SiC-bearing specimens as a function of heat treatment temperature and soaking time, respectively.

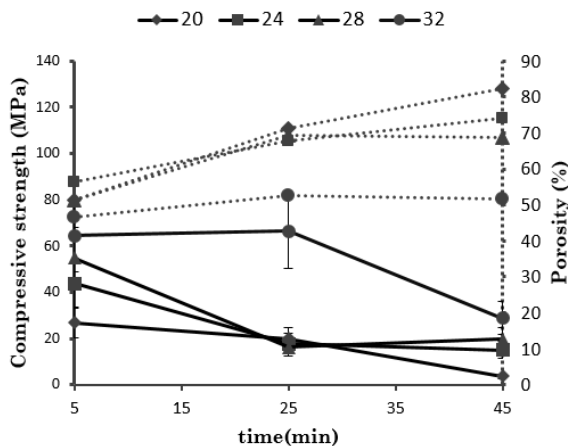


Fig. 10- Strength-porosity variation of specimens with soaking time in the presence of %2wt SiC at 850°C.

According to Fig. 9, while there is not a meaningful difference between the porosity amounts of the specimens fired at 750 °C, the most porosity (90%) and the least one (50%) belong to  $G_{20}$  and  $G_{32}$ , respectively, after heat treatment at 950 °C. Furthermore, except for  $G_{32}$ , the compressive strengths of the other samples are decreased gradually by increasing the porosity with temperature, as expected, from approximately 70 to about 4 MPa. In  $G_{32}$ , increasing the viscosity of the specimen with raising the heat treatment temperature from 850°C to 950°C, due to intensifying of crystallization, however, has retarded the reaction in the glass-SiC interfaces. Consequently, the porosity as well as the strength have been remained nearly constant in this heat treatment temperature interval.

Based on Fig. 10, the heat treatment time did not affect the porosity, and strength of the samples relative to each other and the  $G_{32}$  acted again differently from  $G_{20}$ ,  $G_{24}$ , and  $G_{28}$  with regard to strength and foaming behavior. Accordingly, it can be concluded that there is a threshold of crystallinity above which the foaming process is prohibited. It should also be noted that even the latter glass-ceramic foams show an overall higher strength than the non-crystallized ones investigated in previous studies [2, 8, 9, 11, 13].

Fig. 11(a,b,c, and d) depicts the crushing strengths of various glass-ceramic foams as a function of relative density. It can be seen that the density of specimens  $G_{20}$ ,  $G_{24}$ , and  $G_{28}$  changes almost linearly to higher-value with increasing of their iron oxide. However, there is not such a trend in  $G_{32}$  such that its relative density limited to 0.4- 0.6  $\text{g}/\text{cm}^3$ . Furthermore, the least and most densities belong to  $G_{20}$  and  $G_{32}$ .

The present authors believe that iron oxide has not helped the foaming process of specimens in this work and it solely plays the role of a crystalline constituent that improves the mechanical properties of the specimens. This effect originates probably from the high amounts of it used in the compositions.

Yuwei Chi et al. [28] who have investigated the effects of  $\text{Fe}_2\text{O}_3$  on the properties of glass

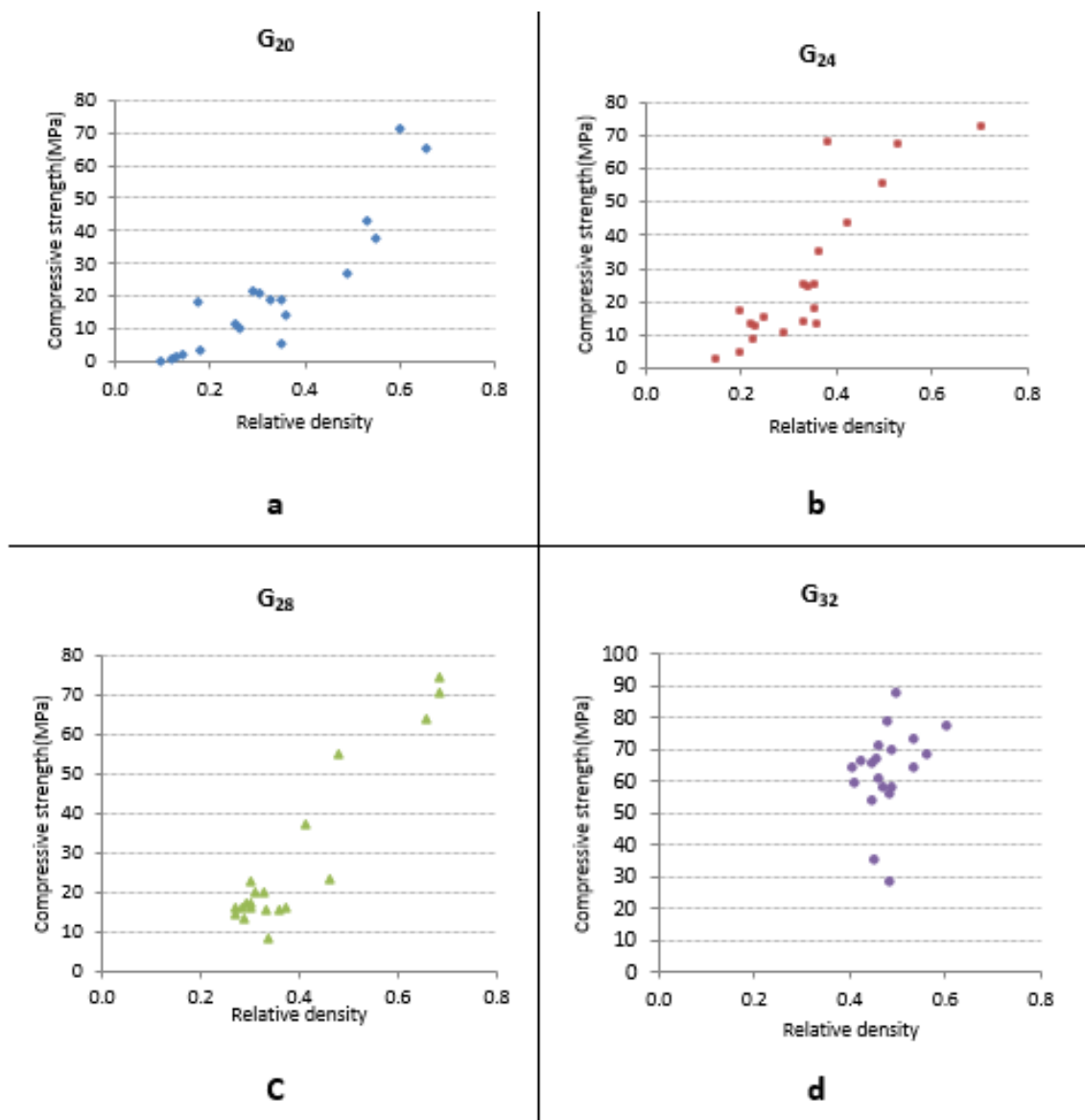


Fig. 11. Plot of Strength vs relative density for a) glass  $G_{20}$  and b) glass  $G_{24}$  c) glass  $G_{28}$  d) glass  $G_{32}$  foams.

foams by using iron-containing solid waste have shown that  $Fe_2O_3$  in glass matrix would increase the viscosity of glass on one hand. On the other hand, they believe an appropriate content of  $Fe_2O_3$  could leading to a better compromise between the glass viscosity and the gas generating, so as to a lower density. Based on their results, adding 1wt. %  $Fe_2O_3$  as oxidants could promote the foaming ability of the specimen and proper utilization of the  $Fe^{3+}$  ions in parent glass would be beneficial to obtain glass foams with better properties. However, Saeedi Heydari et al. [29] who have

used less than 1.2 wt. %  $Fe_2O_3$  as an oxidizer in preparation of glass foam from waste cathode ray tube display panel (CRT) have rejected the role of it as an oxidizer in the glass.

#### 4. CONCLUSIONS

The present work showed that the addition of  $Fe_2O_3$  to the  $SiO_2$ - $Na_2O$ - $CaO$  glass system caused the crystallization of pyroxene solid solution crystals, i.e. diopside and acimte, within the glasses.  $Fe_2O_3$  neither acted as an oxidizer for SiC particles nor a nucleant for crystallization. The pyrox-



ene phase was precipitated in the glass through the surface crystallization mechanism.

Pyroxene based glass-ceramic foams with high compressive strength (20MPa) and desirable porosity (~70%) were prepared using 20 to 28 parts by weight iron oxide, when heat treated at 850°C for 25 min. Using 30 parts by weight iron oxide led to a glass-ceramic with undesirable porosity (45%), but superior compressive strength (60 MPa).

## REFERENCES

1. M., Scheffler, and P., Colombo, Cellular ceramics, Wiley-Vch, 2006.
2. F., Mear, P., Yot, M., Cambon, and M., Ribes, "Elaboration and characterization of foam glass from cathode ray tubes", Advances in applied ceramics, 2005, 104, 123-130.
3. A. C., Steiner, "Foam glass production from vitrified municipal waste fly ashes", 2006, 68, 91-118.
4. A. S., Llaudis, M. J. O., Tari, F. J. G., Ten, E., Bernardo, and P., Colombo, "Foaming of flat glass cullet using Si<sub>3</sub>N<sub>4</sub> and MnO<sub>2</sub> powders", Ceramics international, 2009, 35, 1953-1959.
5. J. P., Wu, A. R., Boccaccini, P. D. Lee, M. J. Kershaw and R. D. Rawlings, "Glass-ceramic foams from coal ash and waste glass: production and characterization", Advances in applied ceramics, 2006, 105, 32-39.
6. E., Bernardo, and F., Albertini, "Glass foams from dismantled cathode ray tubes", Ceramics international, 2006, 32, 603-608.
7. P., Colombo, G., Brusatin, E., Bernardo, and G., Scarinci, "Inertization and reuse of waste materials by vitrification and fabrication of glass-based products", Current Opinion in Solid State and Materials Science, 2003, 7, 225-239.
8. E., Bernardo, "Micro-and macro-cellular sintered glass-ceramics from wastes", Journal of the European Ceramic Society, 2007, 27, 2415-2422.
9. H. R., Fernandes, D. U., Tulyaganov, J. M. F., Ferreira, "Preparation and characterization of foams from sheet glass and fly ash using carbonates as foaming agents", Ceramics international, 2009, 35, 229-235.
10. D. U., Tulyaganov, H. R., Fernandes, S., Agathopoulos, J. M. F., Ferreira, "Preparation and characterization of high compressive strength foams from sheet glass", Journal of Porous Materials, 2006, 13, 133-139.
11. H., Guo, Y., Gong, S., Gao, "Preparation of high strength foam glass-ceramics from waste cathode ray tube", Materials Letters, 2010, 64, 997-999.
12. N. M., Bobkova, S. E., Barantseva, E. E., Trusova, "Production of foam glass with granite siftings from the Mikashevichi deposit", Glass and Ceramics, 2007, 64, 47-50.
13. E., Bernardo, G., Scarinci, P., Bertuzzi, P., Ercole, L., Ramon, "Recycling of waste glasses into partially crystallized glass foams", Journal of Porous Materials, 2010, 17, 359-365.
14. E., Bernardo, R., Cedro, M., Florean, S., Hreglich, "Reutilization and stabilization of wastes by the production of glass foams", Ceramics international, 2007, 33, 963-968.
15. S., Hasheminia, A., Nemat, B. E., Yekta, P., Alizadeh, "Preparation and characterization of diopside-based glass-ceramic foams", Ceramics International, 2011, 38, 2005-2010.
16. E., Mohamed, P., Shahsavari, B., Eftekhari-Yekta and V., K. Marghussian, "Preparation and Characterization of Glass Ceramic Foams Produced from Copper Slag", Trans. Ind. Ceram. Soc., 2015, 74, 1-5.
17. R. K., Singh, G. P., Kothiyal, A., Srinivasan, "Influence of iron ions on the magnetic properties of CaO-SiO<sub>2</sub>-P<sub>2</sub>O<sub>5</sub>-Na<sub>2</sub>O-Fe<sub>2</sub>O<sub>3</sub> glass-ceramics", Solid State Communications, 2008, 146, 25-29.
18. S. M., Salman, S. N., Salama, "Pyroxene solid solutions crystallized from CaO-MgO (Li<sub>2</sub>O, Fe<sub>2</sub>O<sub>3</sub>)-SiO<sub>2</sub> glasses", Ceramics international, 1986, 12, 221-228.
19. P., Alizadeh, B., Eftekhari Yekta, A., Gervei, "Effect of Fe<sub>2</sub>O<sub>3</sub> addition on the sinterability and machinability of glass-ceramics in the system MgO-CaO-SiO<sub>2</sub>-P<sub>2</sub>O<sub>5</sub>", Journal of the European Ceramic Society, 2004, 24, 3529-3533.
20. W., Holand and G. H., Beall, "Glass-ceramic technology, Wiley-American Ceramic Society, Ohio, 2012, 118.
21. V. G., Sister, E. M., Ivannikova, M. A., Semin, and A. A., Egorov, "Preparation of highly porous cellular glass materials in the field of pyroxene crystallization", Chemical and Petroleum Engineering, 2011, 46, 631-633.
22. P. A., Bingham, J. M., Parker, T., Searle, J. M., Williams, K., Fyles, "Redox and clustering of iron in silicate glasses, Journal of Non-Crystalline Solids, 1999, 253, 203-209.
23. S. N., Salama, S. M., Salman, "Crystallization characteristics of iron-containing spodumene-diopside glasses", Journal of the European Ceramic Society, 1993, 12, 61-69.
24. A., Karamanov, M., Pelino, "Crystallization

- phenomena in iron-rich glasses”, *Journal of non-crystalline solids*, 2001, 281, 139-151.
25. Z. j., Wang, W., Ni, K. Q., Li, X. Y., Huang, L. P., Zhu, “Crystallization characteristics of iron-rich glass-ceramics prepared from nickel slag and blast furnace slag”, *International Journal of Minerals, Metallurgy, and Materials*, 2011, 18, 455-459.
  26. I., Levitskii, “The Effect of Iron Oxides on the Properties and Structure of Glazed Glasses”, *Glass and Ceramics*, 2003, 60, 111-114.
  27. B., Eftekhari Yekta, V. K., Marghussian, “Sintering of  $\beta$ . q. SS and gahnite glass ceramics”, *Journal of the European Ceramic Society*, 1999, 19, 2963-2968.
  28. Yuwei Chi Lin, J. and Xu, B., “Effects of  $Fe_2O_3$  on the Properties of Glass Foams Prepared by Iron-Containing Solid Waste”. *Glass Phys. Chem.*, 2019, 45, 104-110.
  29. Saeedi Heydari, M., Mirkazemi, S. M., and Abbasi, S., ”Influence of  $Co_3O_4$ ,  $Fe_2O_3$  and SiC on microstructure and properties of glass foam from waste cathode ray tube display panel (CRT)”, *Journal Advances in Applied Ceramics Structural, Functional and Bioceramics*, 2014, 113, 173-179.